Effect of bismuth surfactant on the structural, morphological and optical properties of self-assembled InGaAs quantum dots grown by Molecular Beam Epitaxy on GaAs (001) substrates

Haifa Alghamdi[1,2], Amra Alhassni[2,8], Sultan Alhassan[2], Amjad Almunyif[2], Alexey V. Klekovkin[3,4], Igor N. Trunkin[5], Alexander L. Vasiliev[5], Helder V. A. Galeti[6], Yara Galvão Gobato[7], Igor P. Kazakov[3], Mohamed Henini[2]

[1]Physics Department, Faculty of Sciences, AL Faisaliah, University of Jeddah, Ministry of Education Kingdom of Saudi Arabia, Jeddah 21959, Saudi Arabia
[2]School of Physics and Astronomy, University of Nottingham, Nottingham NG7 2RD, UK
[3]P.N. Lebedev Physical Institute Russian Academy of Sciences, Moscow 119991, Russia
[4]Institute of Ultrahigh Frequency Semiconductor Electronics of Russian Academy of Sciences, Moscow 117105, Russia
[5]National Research Center "Kurchatov Institute", Moscow 123182, Russia
[6]Electrical Engineering Department, Federal University of São Carlos, 13565-905, São Carlos-SP, Brazil
[7]Physics Department, Federal University of São Carlos, 13565-905, São Carlos-SP, Brazil
[8]Department of Physics, College of Science, Al-Baha University, 65779-77388 Al-Aqiq, Saudi Arabia.

Contact author: hmalghamdi@uj.edu.sa

ABSTRACT

In this work, we have investigated the effect of Bi surfactant on structural, morphological and optical properties of 5 monolayers self-assembled InGaAs quantum dots (QDs) grown on GaAs (001) substrates at various growth temperatures (435, 467 and 495 ºC) by Molecular Beam Epitaxy. Two types of InGaAs QDs samples grown with and without exposure to bismuth were studied using Atomic Force Microscopy, Scanning Electron Microscopy, Transmission Electron Microscopy and Photoluminescence (PL). Our results have demonstrated that Bi-mediated growth provides improved control of several properties of InGaAs QDs including an enhancement of the QD PL peak intensity by 1.7 times as compared to InGaAs/GaAs control sample grown without Bi. In addition, a red-shift of the PL peak energy of about 40 meV was also observed when the InGaAs QDs were grown by using Bi evidencing that Bi surfactant affects considerably the size of QDs. Furthermore, the QDs grown with Bi surfactant exhibited a higher degree of size uniformity as demonstrated by the observation of narrower Full Width at Half Maximum (FWHM) of the PL peaks. We have also shown that both Bi surfactant and substrate temperature play an important role to control the density of InGaAs QDs. The QD density decreased from 8.9×10^{10} cm^{-2} (control sample) to 2.0×10^{10} cm^{-2} for the sample grown at the lowest temperature of 435 ºC under Bi flux. All these approaches to control and improve the properties of self-assembled QDs are important for device applications that require high optical efficiency and low QD density.

INTRODUCTION

Improved control of the QD size, uniformity, and density (all of which affect the QD electronic states) are considered as an important requirement for further progress in QD-based devices. The QD coalescence is one significant problem for epitaxial growth of large InAs QDs since it results in inhomogeneous size, a decrease in density and dislocated QDs, which degrade the QD morphology and optical properties. Different growth parameters have been applied to control the QD density and size including the growth rate, substrate temperature, growth interruptions, and alloy capping layers [1-6]. The increase of the substrate temperature or decrease of the InAs growth rate during QD growth results in larger QDs due to increased adatom diffusion length. However, there is a concomitant decrease in QD density with these approaches. There is another alternative technique to control QD size and density during growth which involves the use of a surfactant [7]. For instance, Antimony (Sb) has been successfully used as a surfactant during the growth of InAs QDs on GaAs, which usually results in smaller QD sizes and increased QD densities [8,9]. Alternatively, bismuth (Bi) is also considered as a good surfactant because the larger Bi atoms do not incorporate into the InAs QDs or the surrounding GaAs matrix when the growth temperature is high. It is important to point out that substitutional incorporation of Bi into the host lattice of III-V compounds requires low temperature growth (< 400 °C) [35,36]. It is, therefore, becoming an excellent candidate for solving the QD coalescence problem and improving the PL intensity of heterostructures grown epitaxially [10-12]. Previous studies on surfactant-mediated epitaxial film growth revealed that at typical growth temperatures, Bi segregates to the surface without incorporating into the epilayer and acts as a reactive surfactant to kinetically limit the surface adatom mobility and improve surface smoothness [13-15]. Moreover, bismuth is an efficient surfactant in Molecular Beam Epitaxy (MBE) growth of InGaAs at low temperatures [16]. On the other hand, only few studies about the influence of Bi on InAs QDs have been reported in the literature [10-12, 18-21] while Bi mediated growth of InGaAs QDs remain unexplored.

Intense investigation has been dedicated to understand whether Bi decreases or increases the surface migration of indium (In) adatoms during the growth of InAs QD. It was reported that Bi can kinetically limit the surface adatom mobility and decreases the In adatom diffusion length and thus increases the QD density [10, 17]. It was shown that InAs QDs grown with Bi with a critical thickness of 2.6 monolayers (MLs) have a smaller density than samples grown without Bi thicknesses <2.6 MLs. For thicknesses >2.6 MLs the QD density with Bi exceeded those grown

without Bi. On the other hand, an opposite effect of Bi on the QD density and dimension were observed [12]. Chen et al studied the effect of the growth temperature of self-assembled InAs QDs grown on GaAs substrates with and without exposure of bismuth surfactant [18]. The results indicated that the coalescence amongst InAs QDs was significantly inhibited by the exposure of bismuth flux during growth in the temperature range 475 - 500 °C, resulting in a modified dot density and improved dot uniformity. The use of Bi as surfactant has been shown to suppress the surface migration and desorption of In adatoms during the growth of InAs QDs [6, 12, 16, 18]. This suppression mechanism leads to a suppression of coalescence and ripening of InAs QDs. It was shown that as the growth temperature increases in the absence of Bi surfactant, the dot density decreases but resulted in large and defective InAs islands. By contrast, for the Bi-mediated growth, the dot areal density increased at high growth temperatures [17] but decreased at low temperatures [12]. This finding confirmed the suppression effect of Bi on the surface migration and desorption of In adatoms. Additionally, at higher growth temperatures the QD size uniformity improved since the presence of Bi atoms suppresses the formation of larger dislocated islands.

In this work, we investigated the effect of Bi surfactant on the growth of self-assembled InGaAs QDs deposited on GaAs (001) substrates at various temperatures. We have shown that both Bi surfactant and substrate temperature play an important role to control the density of InGaAs QDs and improve their optical properties. InGaAs QD samples were grown on GaAs (001) substrates with and without (control samples) Bi surfactant. Our experimental results demonstrate that Bi-mediated growth provides improved control of InGaAs QDs, by not only decreasing the density of InGaAs QDs but also resulting in an enhancement of the PL intensity and a red-shift of PL peak energy, which are very important properties for applications that require high optical quality and low QD density. Finally, our studies provide an alternative for the growth of novel laser nanostructures based on 0D/2D dimensionality that we refer to as quantum well-dots (QWDs) [22].

EXPERIMENTS

All samples investigated in this work were grown by MBE using solid sources on semi-insulating GaAs (001) substrates. The layer structure of the grown samples is presented in Figure 1(a-d). After desorption of the oxide layer from the substrate surface, a 160 nm undoped GaAs buffer layer was deposited at a growth temperature (T_G) of 630°C with a rate of 0.19 nm/s. For sample A (control sample without Bi), the substrate temperature was ramped down from 630°C to 495°C for the formation of InGaAs QDs by growing ~ 5 MLs of InGaAs by pulse deposition InAs (1s)/GaAs (1s) x 8 at a beam equivalent pressure

(BEP) of In, Ga, and As_4 of 3.6 x 10^{-7}, 1.7 x 10^{-7}, and 2.5 x 10^{-6} Torr, respectively. A 100 nm undoped GaAs capping layer was grown at the same temperature of 495°C. Finally, the same InGaAs layer was grown on top of the GaAs cap layer for structural analysis (see Figure 1(A)). During the temperature T_G ramping down to 495 ºC over a period of 400 s, GaAs was impulse deposited 4 times with a 5 s duration in order to refresh the surface. The composition of In was determined by X-ray diffraction analysis on specially grown 100 nm thick $In_xGa_{1-x}As$ epitaxial layers on InP substrates with similar BEP. InP substrate was chosen because it is lattice matched to $In_{0.52}Ga_{0.48}As$. The growth temperature was measured with an accuracy of ±5 ºC using a thermocouple located at the back of the substrate holder and an infrared pyrometer Mikron M680, which was used to determine the changes in the temperature of the substrate at various moments during the transient processes of the growing films. The calibration of the GaAs substrate temperature was carried out using temperature reference points, determined by RHEED which is one of the most common tools used in MBE to calibrate surface temperatures: the amorphous Arsenic (As) desorption temperature (250 ^{0}C) and transition of surface reconstruction from (4x4) → (2x3) → (2x4) → (3x6) → (4x2), observed during heating of the substrate in the absence of As fux at temperatures of 354, 395, 500, 549 ^{0}C, respectively [37].

To investigate the effect of Bi exposure on $In_xGa_{1-x}As$ QDs, the deposition of $In_xGa_{1-x}As$ layer was carried out using an additional Bi flux with a BEP of 4.5x10 $^{-8}$ Torr for the growth of sample B (T_G = 495 ºC), sample C (T_G = 467 ºC) and sample D (T_G = 435 ºC), as shown in Fig 1b, Fig 1c and Fig 1d, respectively. The 100 nm undoped GaAs capping layer was grown at the same growth temperature with the Bi source closed (see Figure 1 (b, c, d)). It is important to point out that the Bi source was opened 30s before the deposition of both $In_xGa_{1-x}As$ layers (the buried layer and the top layer).

The flux of Bi atoms to the substrate surface was measured using a control $GaBi_x As_{1-x}$ (50 nm)/GaAs sample grown at a temperature of 285 ^{0}C, when no re-evaporation of Bi from the GaAs surface occurs [38]. For the MBE growth of our structures, the Bi and Ga BEP of 4.5x10 $^{-8}$ Torr and 6x10^{-8} Torr, respectively, were chosen with the aim to increase the incorporation of Bi into the GaAs host lattice, and hence the content of Bi. The Bi composition, as determined by XRD from the main volume of the grown $GaBi_x As_{1-x}$ layer, was x = 0.105. This made it possible to estimate the flux of Bi atoms to the substrate surface during the growth of $In_xGa_{1-x}As$ QDs as 5.8x10^{12} at./cm^2/s. The flux of group III atoms during QD growth was about 1.1x10^{14} at./cm^2/s, i.e., the flux ratio was Bi/III ≈ 0.05. In addition, it is essential to note that there is no Bi incorporation in our samples since Bi does not incorporate into the host lattice of GaAs and InAs for growth temperatures above ~440 ºC [35,36]. We performed elemental analysis in our samples

using energy dispersive X-rays spectroscopy (EDX), which confirmed the absence of Bi incorporation.

The growth process was controlled by Reflection High Energy Electron Diffraction (RHEED). The morphology of the samples surface was investigated by Atomic Force Microscopy (AFM) SOLVER P47-SPM-MDT, Scanning Electron Microscopy (SEM) JEOL 700 1F. For the examination of samples by Transmission Electron Microscopy (TEM) and scanning transmission electron microscope (STEM), cross-sectional specimens were prepared by standard polishing and ion beam thinning. After mechanical thinning to a thickness of 20–40 μm, the samples were thinned by 5-keV Ar+ ions on a Gatan 691 system (GATAN, United States) until a hole was formed. The final polishing was performed by Ar+ ions with energy reduced to 0.1 keV. The heterostructures were investigated using a TITAN 80-300 (ThermoFisher Scientific, Waltham, Massachusetts) with a spherical aberration corrector in bright field (BF) and high angle annular dark field (HAADF), respectively, modes at an accelerating voltage of 300 kV. Image processing was performed with TIA (FEI) and Digital Micrograph (Gatan, Pleasanton, California) software.

Photoluminescence (PL) spectra of all samples were investigated as a function of laser power and temperature using a Janis closed-loop helium cryostat. The samples were excited with a 532 nm Nd:YAG solid state laser. The PL signal was collected in a Andor Shamrock 500i spectrometer coupled with a high sensitivity Andor iDus InGaAs CCD camera. The PL spectra in the figures below are presented using both logarithmic scale or linear scale in the intensity axis in order to evidence different effects.

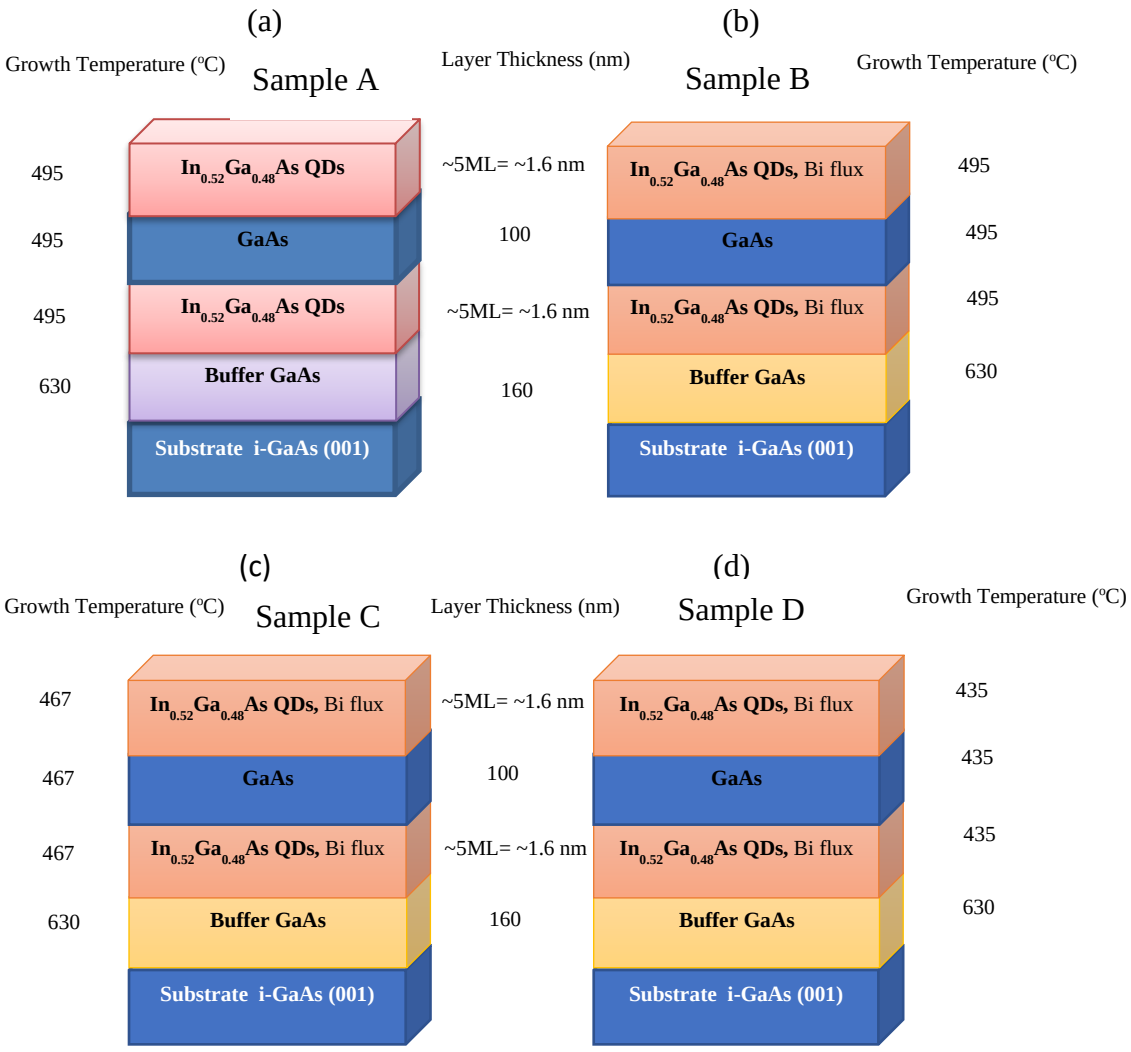

Figure 1: Schematic diagram of $In_{0.52}Ga_{0.48}As$ QDs samples grown with and without Bi surfactant at different growth temperatures (T_G): (a) samples grown without Bi surfactant (T_G = 495 ºC); samples grown with Bi surfactant at (b) T_G = 495 ºC, (c) T_G = 467 ºC and (d) T_G = 435 ºC. The Bi surfactant source was switched on only during the growth of the top and inner $In_{0.52}Ga_{0.48}As$ QDs layers of samples B, C and D.

RESULTS AND DISCUSSION

RHEED

Preliminarily, before growing samples A-D, RHEED experiments were carried out to monitor the pulse deposition of 5 MLs $In_{0.52}Ga_{0.48}As$ layers on GaAs buffer layer at same BEP, but at different temperatures. After the growth of the GaAs buffer layer for all samples, a typical

diffraction pattern was observed, which is characteristic of a (2x4) surface reconstruction as shown in Fig. 2a.

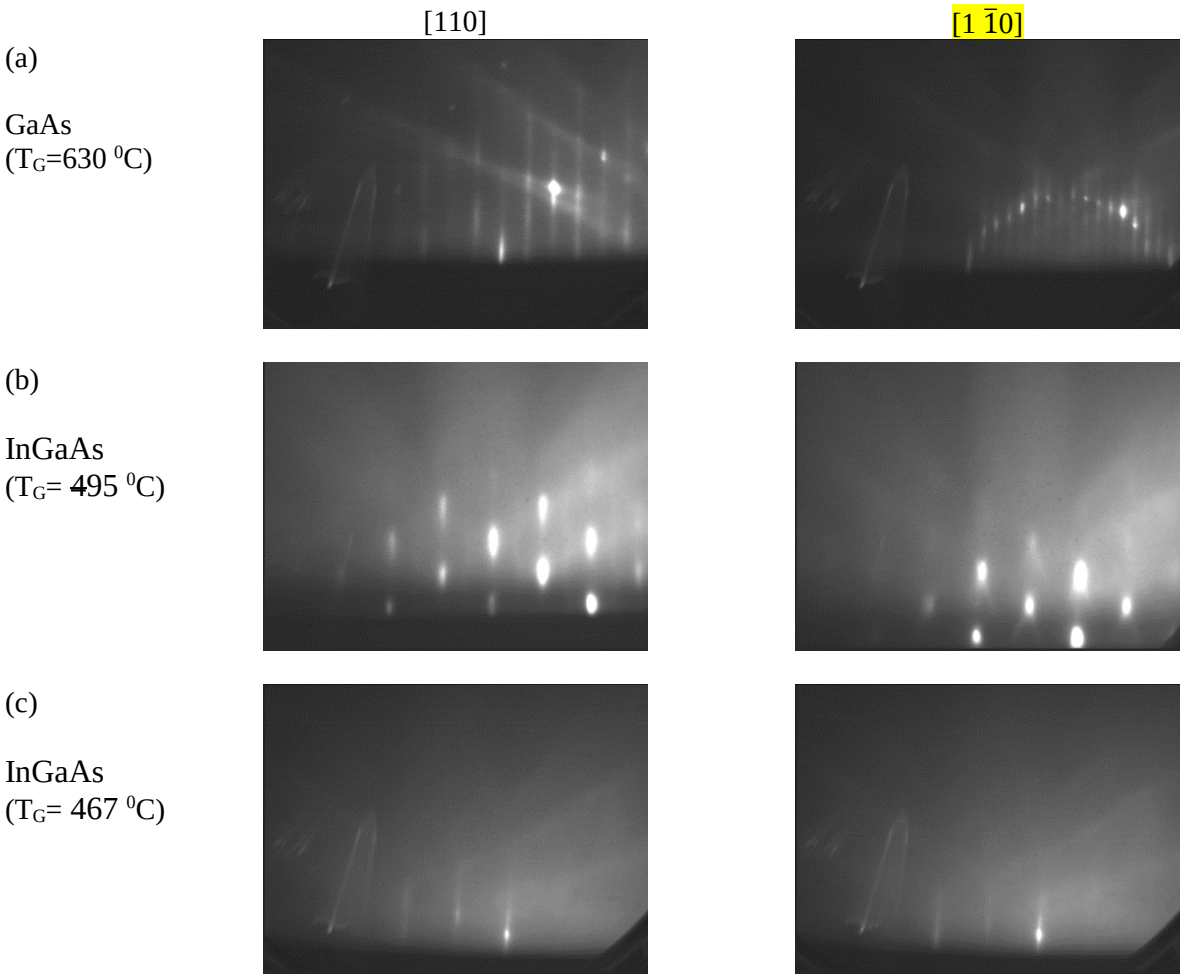

Figure 2: RHEED patterns in azimuths [110] and [1 $\bar{1}$0] [from the initial GaAs surface (a) and 5 MLs $In_{0.52}Ga_{0.48}As$ layers (b, c) grown at different substrate temperatures T_G without Bi flux. At a temperature T_G of 467 ^{0}C (c), the formation of QDs is not observed. The samples were grown at T_G (a) 630 ^{0}C, (b) 495 ^{0}C, and (c) 467 ^{0}C.

As can be seen from Fig. 2(b), for a temperature T_G = 495 ^{0}C the RHEED pattern on the surface of the $In_{0.52}Ga_{0.48}As$ layer becomes spotty, however, for a T_G of 467 ^{0}C only a slight cloudiness of the pattern was observed with preservation of elongated reflexes (Fig. 2(c)). The transition from extended reflections to point reflections (Fig. 2 (b)) indicates a 2D to 3D surface transformation, and the high brightness of point reflections to insignificant stresses in the $In_{0.52}Ga_{0.48}As$ layer. In contrast, the presence of elongated reflexes ((Fig. 2 (c)) indicates that the surface remains

smooth, and the blurring of the picture is a sign of residual stresses as a result of difficult relaxation. Thus, it was found that under these growth conditions, at T_G of 495 ^{0}C, relaxation of the lattice mismatch stresses of GaAs and $In_{0.52}Ga_{0.48}As$ occurs due to the 2D to 3D surface transformation, and at T_G 467 ^{0}C there is no significant relaxation.

It is important to point out that the diffraction patterns observed from the $In_{0.52}Ga_{0.48}As$ QDs top layers of samples B, C and D grown under a Bi flux (Fig. 3), were significantly different from those preliminarily grown $In_{0.52}Ga_{0.48}As$ samples layers. The formation of 3D islands was observed at all growth temperatures (samples B, C and D). In all diffraction patterns, there are additional reflections from the reconstruction (2x3), which is characteristic of the growth of GaAs in the presence of Bi flux [23]. It can be seen from Fig.3 that the formation of 3D islands is strongest at a growth temperature of 495 ^{0}C (Fig. 3(a)) as evidenced by the brightest spotty pattern. As the growth temperature T_G decreases, the diffraction pattern becomes less and less spotty and streakier (Fig. 3(b) and (c)).

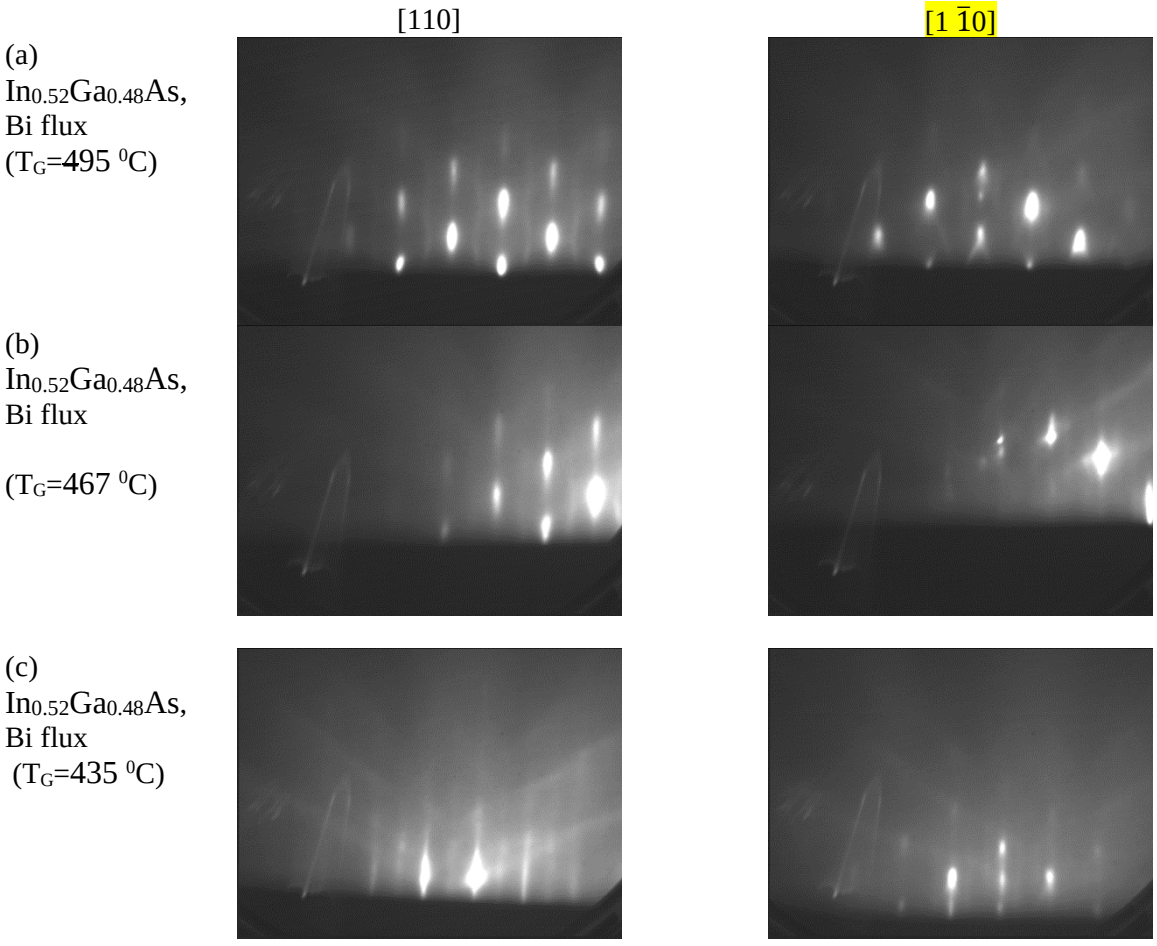

Figure 3: RHEED patterns in azimuths [110] and [1 $\bar{1}$0] of the top $In_{0.52}Ga_{0.48}As$ QD layers grown under a Bi flux at various temperatures T_G: (a) 495 ^{0}C (sample B), (b) 467 ^{0}C (sample C) and (c) 435^{0}C (sample D)

AFM and SEM

The surface morphology of the top $In_{0.52}Ga_{0.48}As$ layer of samples grown without Bi (sample A) and with Bi (samples B, C and D) was significantly different. On the surface of samples A (Fig. 4) and C (Fig. 7) classic QDs formed, while for sample B (Fig. 5) mostly paired QDs were observed. Aggregates from lateral associations of QD [24] with a number of QDs from 2 to 8 occurred in sample C (Fig. 6).

(a)

(b)

(c)

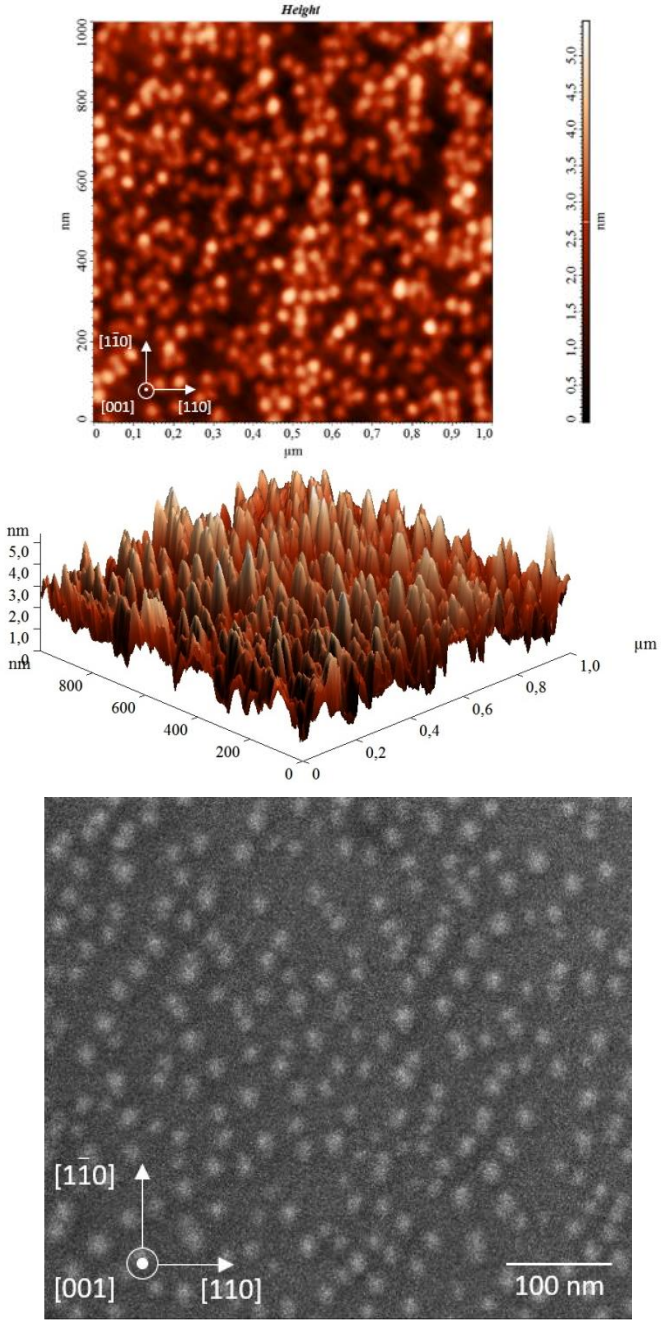

Figure 4: 2D and 3D AFM images of sample A (a, b) 1x1 µm^2 scan, (c) SEM image.

(a)

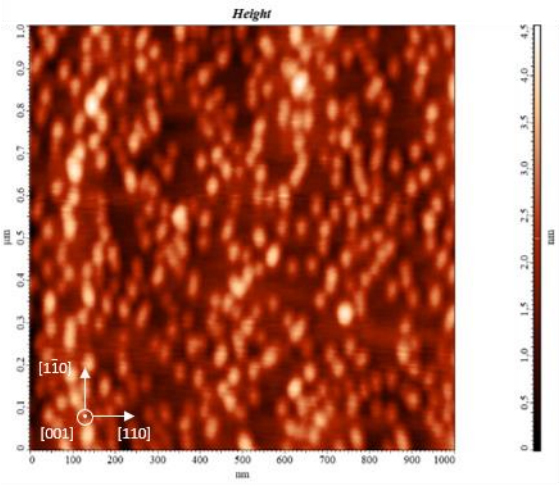

(b)

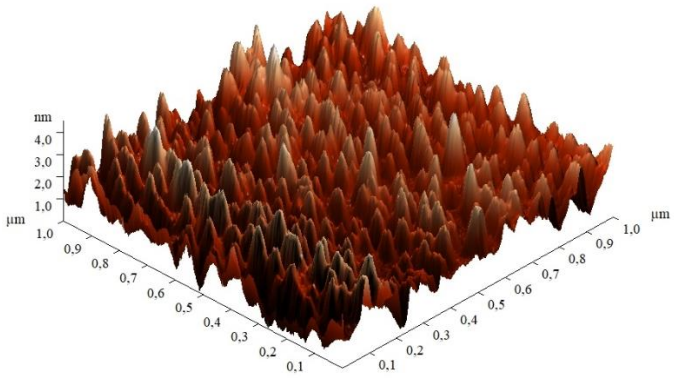

(c)

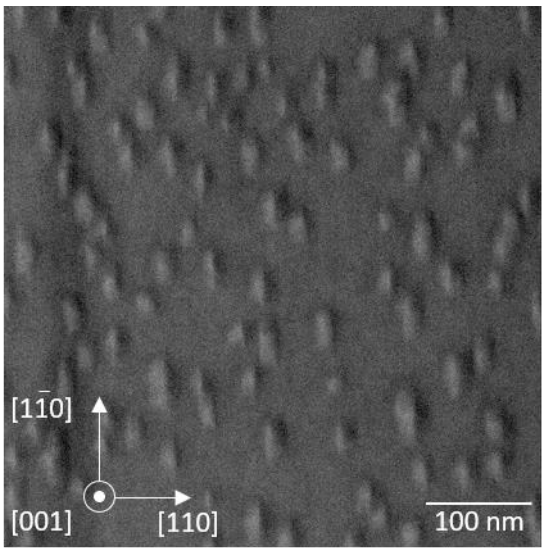

Figure 5: 2D and 3D AFM images of sample B (a, b) 1x1 µm^2 scan, (c) SEM image.

(a)

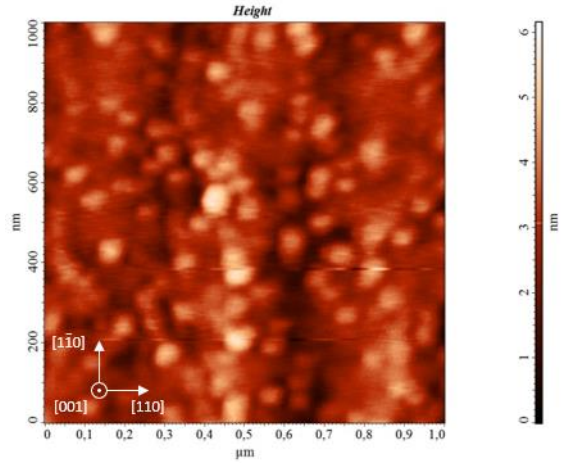

(b)

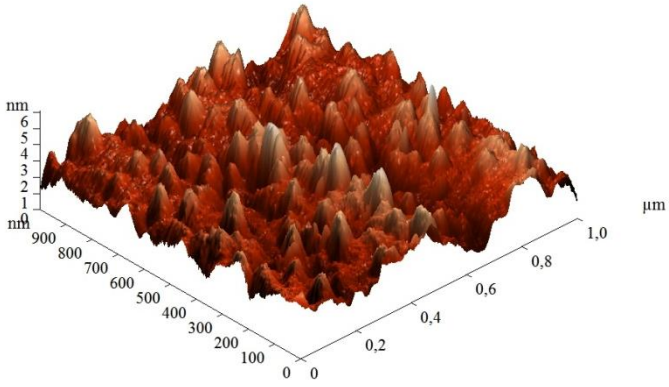

(c)

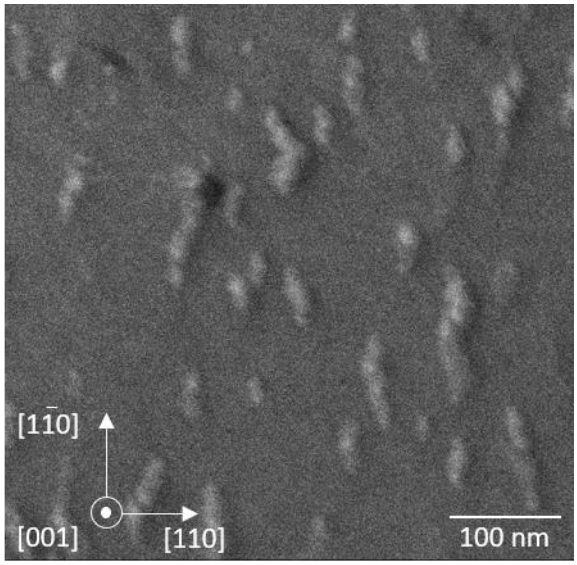

Figure 6: 2D and 3D AFM images of sample C (a, b) 1x1 µm^2 scan, (c) SEM image.

(a)

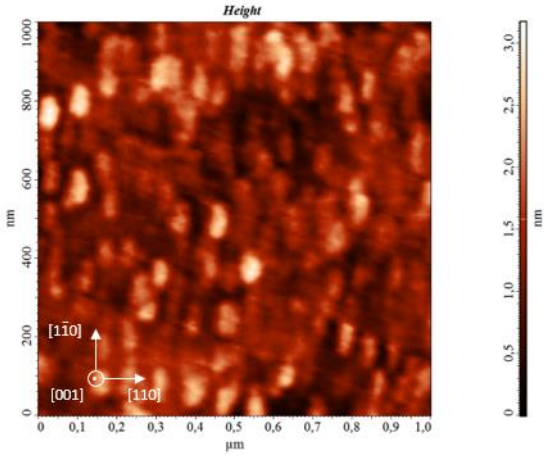

(b)

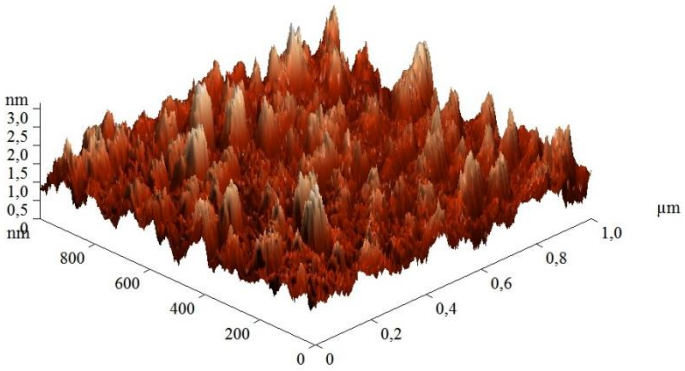

(c)

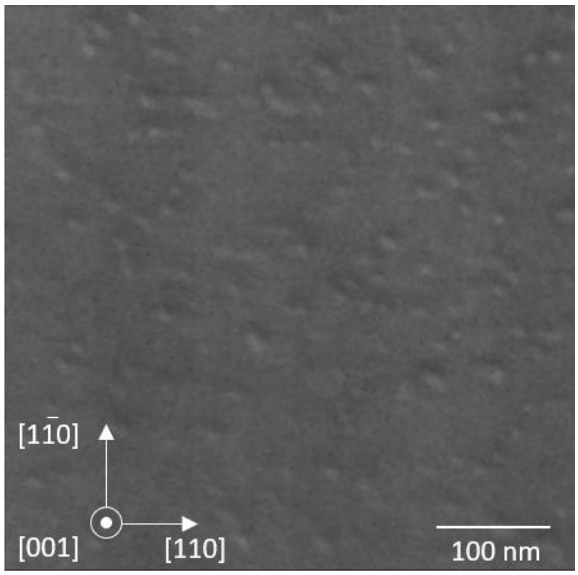

Figure 7: 2D and 3D AFM images of sample D (a, b) 1x1 µm^2 scan, (c) SEM image.

The obtained values of the QDs' density of samples A, B, and C were 8.9x10^{10} cm^{-2}, 6.2x10^{10} cm^{-2}, 3.6x10^{10} cm^{-2}, respectively. The density of QDs for sample D is difficult to determine due to their low height (Fig. 8(e)) and is approximately equal 2x10^{10} cm^{-2}. It is important to point out that when calculating the density, individual QDs in the lateral

associations of QD aggregation were taken into account. For example, if there were 3 QDs in the aggregation, then it was considered "3 QDs" and not "1 QD".

The QD height and its distribution in the samples differed significantly, as can be seen from Fig. 8. The highest QDs, up to 4.5 nm, were observed in samples A and C (Fig. 8 a, c), and the lowest, up to 2 nm, were observed in sample D (Fig. 8 d). The height distribution had the following characteristic features depending on the sample: A - the widest, B - close to bimodal, C - with pronounced features due to ML discreteness, D - the narrowest.

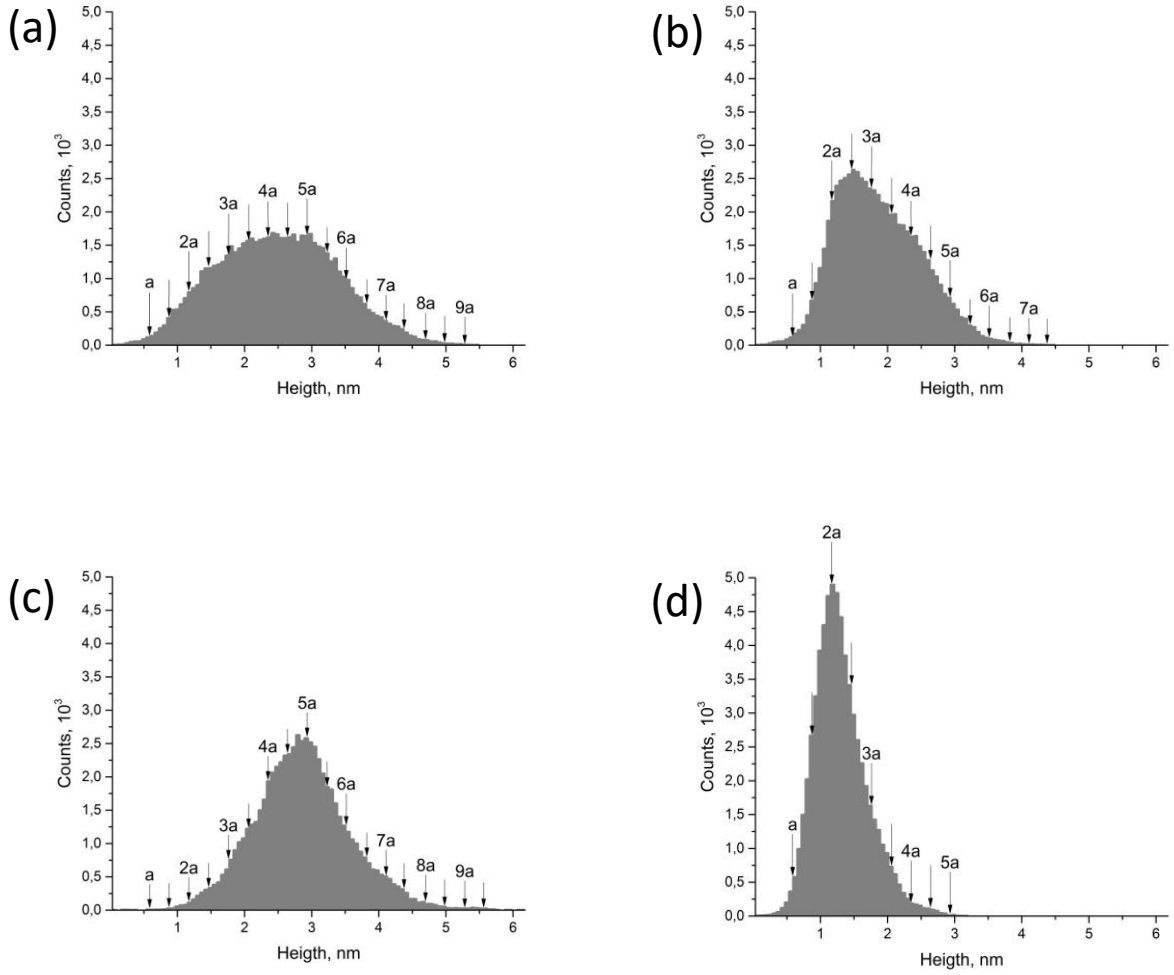

Fig. 8. Histograms of the distribution of QD heights for samples grown (a) without Bi (sample A); and with Bi: (b) sample B, (c) sample C, (d) sample D. The arrows indicate the values of the QD height in units of ML. The lattice parameter of $In_{0.52}Ga_{0.48}As$ is a = 2MLs= 0.586 nm.

TEM

Cross-sectional TEM measurements confirm the presence of InGaAs QDs on the surface of all samples (Fig. 9). No extended defects were found.

(a)

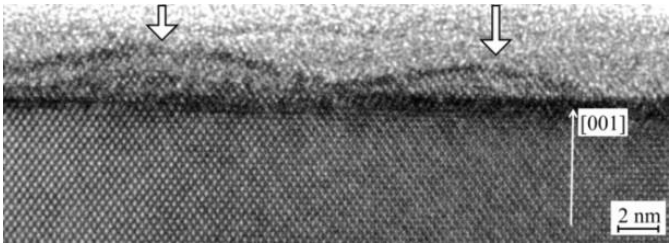

(b)

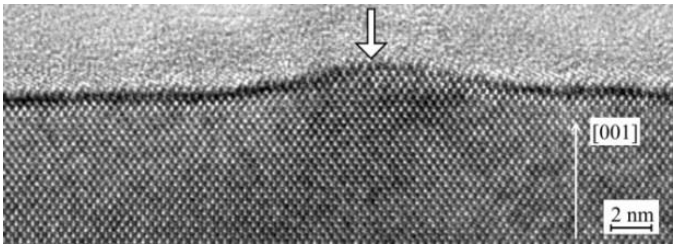

Figure 9: Cross-sectional TEM images of $In_{0.52}Ga_{0.48}As$ QDs top layer of samples A (a), C (b). QDs are indicated by arrows.

The structures of the buried layers of $In_{0.52}Ga_{0.48}As$ were significantly different than those at the surface. In sample A, InGaAs QW with modulated thickness was observed (Fig. 10a). Samples B (Fig. 10b) and D (Fig. 10d) contain both QWs and QDs. In sample C both QW and aggregates from lateral associations of QD were observed (Fig. 10c).

(a)

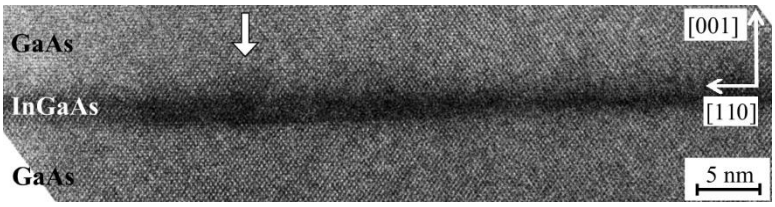

(b)

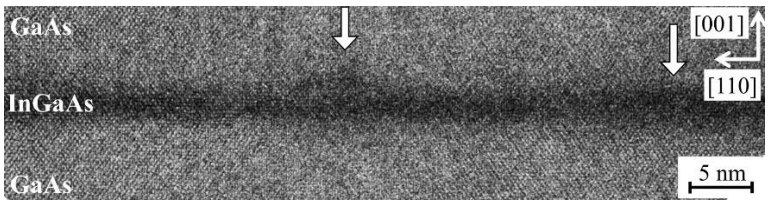

(c)

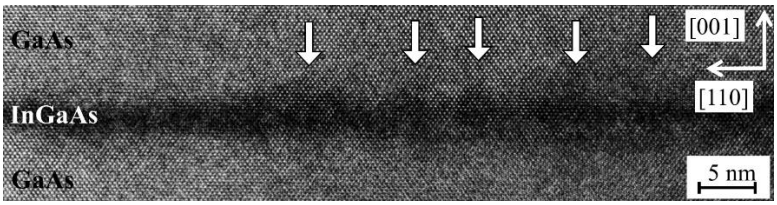

(d)

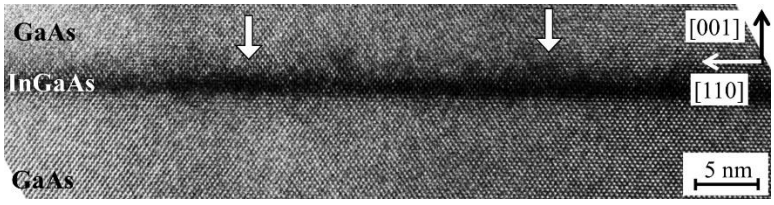

Figure 10: Cross-sectional TEM images of buried $In_{0.52}Ga_{0.48}As$ QDs layer of samples A (a), B (b), C (c) and D (d). It is clearly seen that there is modulation of the layer thickness. Areas of increased thickness are indicated by arrows.

DISCUSSION

The (2x3) reconstruction, which is visible on the surface of the $In_xGa_{1-x}As$ QDs layers of all samples grown under a Bi flux (Figure 3 in manuscript), is intermediate in the transition from the (2x1) reconstruction, usually observed during the growth of $GaBi_xAs_{1-x}$, corresponding to 1 atomic layer of Bi on the GaAs surface, to the static one, namely the (4x3) surface reconstruction [23]. If we assume that the phase diagrams of the surface of $GaBi_xAs_{1-x}$ and GaAs with the $In_xGa_{1-x}As$ wetting layer, on which our QDs were grown under a Bi flux, do not differ much, then we can conclude that the surface concentration of Bi on the wetting layer is high (about 1 atomic layer), which, taking into account the ratio Bi/III ≈ 0.05 determined above, indicates a strong segregation of Bi during the growth. When the GaAs surface was exposed to Bi flux before QD deposition for 30s, about 0.6 atomic layer of Bi could be deposited, assuming that it does not re-evaporate. This made it possible to perform the formation of QDs in the presence of Bi on the surface and, at the same time, exclude the possible formation of its droplets.

From AFM, SEM and TEM results shown above, it is clear that Bi flux has strong effect on the MBE growth process of nanostructures. The growth temperature and the presence of Bi flux have a strong dependence on the morphology of the top InGaAs layer at the surface. In sample A (control sample grown without Bi), classic QDs were formed (Fig. 4), while for sample B, grown at the same temperature but under a Bi flux, mostly paired QDs were observed (Fig. 5). With a decrease in the growth temperature of samples grown with a Bi flux, the tendency towards the coalescence of QDs became more important: in sample C, lateral associations of QD aggregates were observed (Fig. 6). With a further decrease in temperature for the growth of sample D, single QDs, but of a smaller size, again prevailed (Fig. 7).

It should be noted that compared with previously reported results [24], in our work lateral associations of QD are formed at a temperature of about 100^0 C higher, which is caused by the influence of Bi flux on the growth processes. This opens up new possibilities for reducing the concentration of point defects in lateral associations of QD nanostructures.

Interestingly, in addition to the MBE method, annealing procedures were used to obtain lateral associations of QD [25], which are characterized by reduced diffusion of atoms over the surface, as in the case of low-temperature growth in MBE [24] using Bi as a reactive surfactant to reduce surface diffusion. Thus, it can be concluded that for the formation of lateral associations of QD the condition of a low surface diffusion rate is necessary, and the use of Bi opens up new opportunities for controlling the process of their growth.

The values of the QD height on the surface of the samples and the shape of their distribution curve (Fig. 8) significantly depended on the growth conditions. It can be seen that, when the samples were grown in the presence of Bi flux, the distribution of QDs height was significantly narrowed. Noteworthy is a certain correlation of the features in the histograms of heights that are ML discreteness of the InGaAs solid solution, which is especially noticeable in sample C (Fig.8c). The shape of the QD height distribution curve of sample B, a tendency towards bimodality was observed, which can be explained by the formation of “molecules” from

two QDs and the redistribution of mass between them due to the growth of a larger QD due to a smaller one (Ostwald ripening). The same process is observed in sample C, however, lateral associations of QD aggregates contain several QDs, and therefore the height distribution increased.

For the buried QDs in all samples, there was an intermixing between InGaAs and GaAs. Similar effects of QD transformation were studied by Scanning Tunneling Microscopy (STM) [26]. It is important to note that, in contrast to sample A, where QWs with modulated thickness were formed, samples B, C, and D grown under a Bi flux showed nanostructures containing QW and QD - well-dots (QWD). This new type of mixed (0D/2D) dimensionality nanostructures is promising for the creation of microlasers [22].

PHOTOLUMINESCENCE

Figure 11(a) shows typical PL spectra at 10 K with laser power excitation P_{EXC} = 45mW corresponding to power density of 2.55 W/cm^2 for control sample A (InGaAs/GaAs) QDs grown without Bi. The main peak at 1.36 eV with FWHM of ≈ 29.3 meV exhibits some asymmetry toward the low-energy side. A clear and sharper PL peak was also observed in high energy, around 1.40 eV. The high-energy one is attributed to the electron-hole recombination in the wetting layer (WL), whereas the main and lower energy emission are related to the QD ensemble luminescence, in agreement with the AFM and TEM results obtained for this sample (Fig. 4 and Fig. 10), where classical QDs formation were evident, and with previously reported results on MBE-grown InGaAs/GaAs QD structures [27, 28]. In addition, a small peak at 1.492 eV is attributed to the GaAs capping layer/substrate.

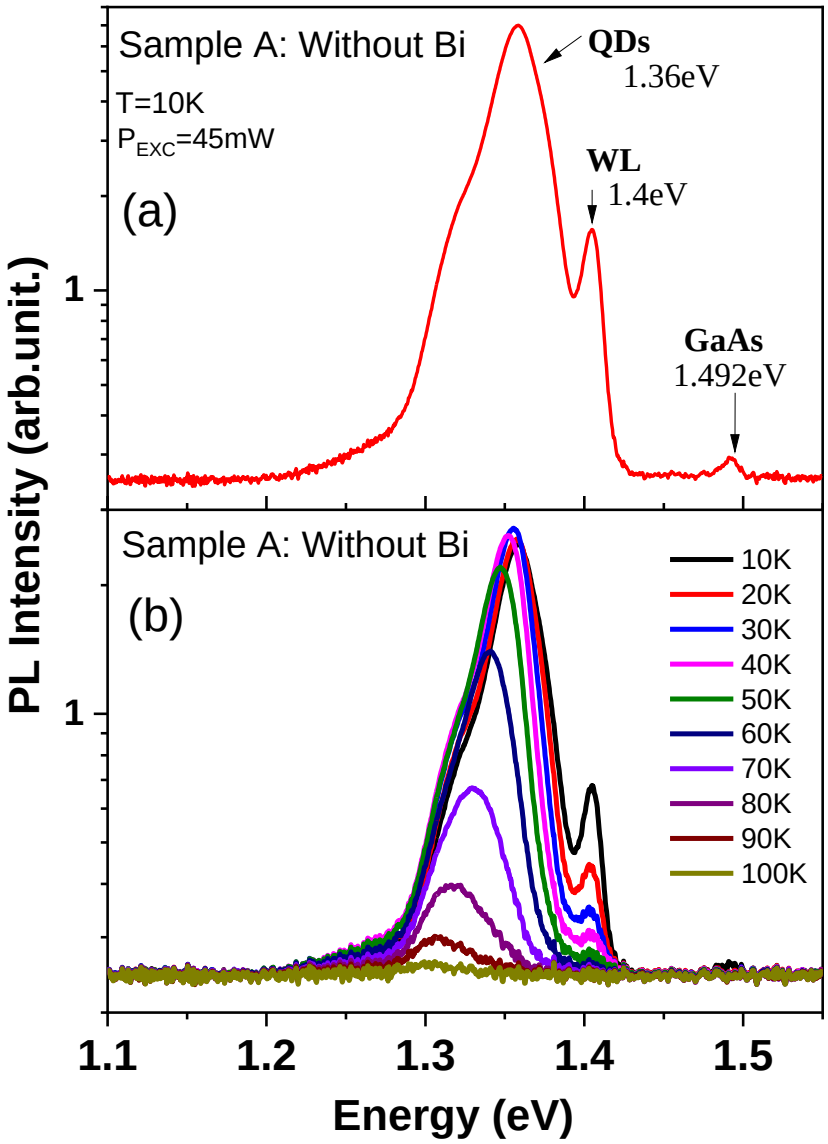

Figure 11: (a) Typical 10K PL spectra (logarithmic scale) for laser power P_{EXC}=45mW. The PL bands attributed to QDs, WL and GaAs substrate are indicated; (b) Typical PL spectra as function of temperature for laser power P_{EXC}=16mW and for $In_{0.52}Ga_{0.48}As$ QDs sample grown without Bi (Sample A).

Figure 11(b) shows that the QD PL intensity increases in the temperature range of 10K to 30K and decreases in the range of 30-100 K, while the WL emission intensity only decreases with increasing temperature. This behavior indicates that the recombination process involves two

different sets of radiative states in the WL and QD, where a temperature-activated carrier transfer process take place. On the other hand, the PL peak position of WL is almost constant (1.40 eV) in the temperature range 10-100 K, whereas for the QD emission peak there is a continuous red-shift. The red shift of QD PL peak and PL intensity dependence as temperature increases could be due to an increase of radiative recombination from the larger QDs as temperature increases. The carriers mainly occupy large QDs at lower temperature. These larger QDs may exhibit some tail states which could act as nonradiative recombination centers. At lower temperatures the photogenerated carriers recombine nonradiatively from the unoccupied tail states. As the temperature increases, these tail states could be occupied by thermally generated carriers, hence the photogenerated carriers recombine primarily radiatively from the InGaAs QD extended states.

Figure 12 shows a comparison of PL spectra at 10K between $In_{0.52}Ga_{0.48}As$ QDs grown without (sample A) and with Bi surfactant (sample B). The effect of Bi surfactant is clearly demonstrated by the following observations: (i) the QD PL peak red-shifted from 1.36 eV to 1.32 eV probably due to the presence of paired QDs which could reduce the quantum confinement, (ii) the PL peak intensity increased its magnitude by 1.7 times, (iii) the FWHM decreased from 29.28 meV to 26.80 meV and (iv) no signal due the WL was detected in sample B.

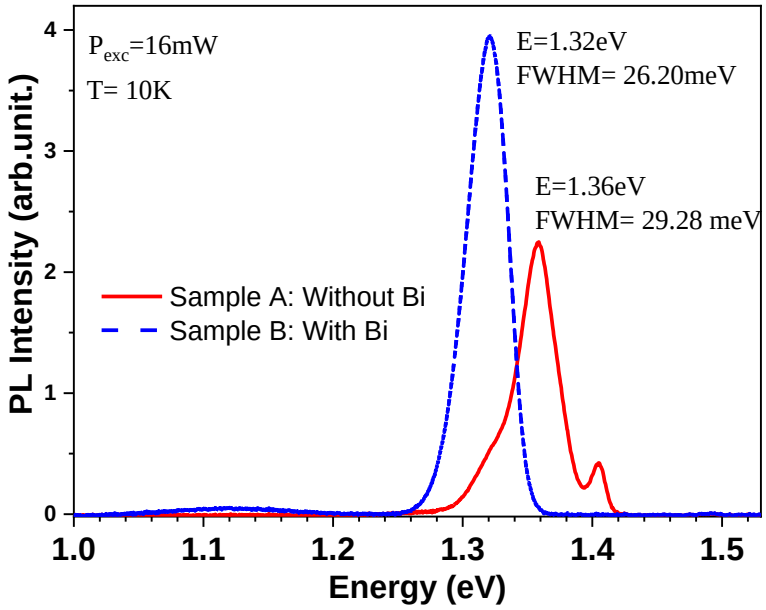

Figure 12: PL spectra from $In_{0.52}Ga_{0.48}As$/GaAs QDs grown without Bi (sample A) and with Bi (sample B) at laser power P_{EXC}=16mW and 10K.

As can be seen in Figure 12 the PL peak position of the ground state emission of the InGaAs QDs grown with Bi (sample B) as surfactant red-shifted with respect to the sample that was not exposed to Bi flux (sample A). Similar results were reported for Bi-mediated growth of InAs QDs [19], which were explained by the fact that QDs are expected to have a lower confinement width due to their dissolution during the capping process [29, 30]. However, the presence of Bi atoms can influence this process by suppression of QD dissolution and then increase the size of resulting QDs, which is a similar effect that was observed when using Sb atoms as surfactant [31,8]. An increase of size of InGaAs QDs in the top layer on the surface was observed in AFM data for sample B as compared to sample A, where the QDs have paired resulting in bimodal shape and uniform size distribution, despite the fact that the distribution of QD height was significantly narrowed. As a result, the red-shift of the PL energy observed in sample B can be explained by a decrease of the quantized energy for this structure. Although one could speculate about the possible formation of a bismuth-containing alloy, such as InAsBi

which has a smaller energy gap than InAs, to explain the PL-peak redshift as reported previously, it is most probable that this effect could be attributed to a decrease in the surface energy caused by Bi surfactant [11].

Additionally, the increase of the PL intensity of sample B indicates that the density of defects which act as nonradiative recombination centers was reduced by supplying Bi at a growth temperature of 495 ^{0}C, while the reduction of the FWHM confirms a more uniform QD size distribution for this sample, which is evident from the AFM size histograms shown in Fig. 5 and Fig. 8(b) as well as the reduction of the QD density ($6.2 \cdot 10^{10}$ cm^{-2}) as discussed in previous section. Therefore, the use of Bi as a surfactant can result a profound impact on the morphology and optical properties of InGaAs QDs. This finding is consistent with previous studies [18, 12, 32] where Bi was confirmed to be an excellent surfactant in InAs QDs growth.

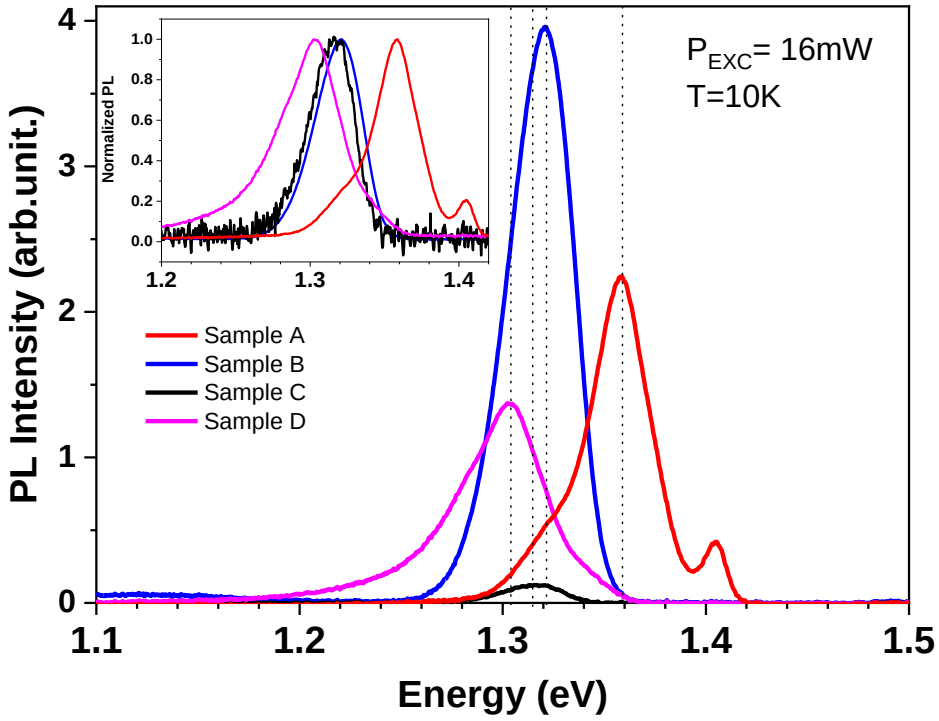

Figure 13: PL spectra from $In_{0.52}Ga_{0.48}As$/GaAs QDs grown at different temperatures using Bi as surfactant: sample B (T_G=495 ^{o}C), sample C (T_G=467 ^{o}C) and sample D (T_G=435 ^{o}C) measured at

10K and a P_{EXC}=16mW. Sample A (control sample without Bi) grown at T_G=495 ºC. The inset figure shows the normalized PL spectra (linear scale).

Figure 13 shows the PL spectra at 10 K with a laser power excitation of P_{EXC} =16mW (0.91 W/cm^2) maybe you could add here the laser power intensity as well) for three QDs samples grown at different temperatures using Bi as surfactant (samples labelled B, C and D) and the QD control sample grown without Bi at T_G=495 ºC (Sample A) for comparison purposes. As observed in Figure 13, when the growth temperature decreased from 495 ºC to 435 ºC, the PL peak position of QDs shifted to lower energies. Particularly, the PL peak energy is observed around 1.320 eV, 1.314 eV and 1.303 eV for sample B, C and D, respectively. The inset in Figure 13 represents the normalized PL spectra. Additionally, it is noticeable that the QD PL intensity of InGaAs/GaAs QDs deposited at a temperature of 467 ºC (sample C) has the smallest intensity.

Similar results were reported in the literature for InAs/GaAs QDs [18] grown at 475 ºC, 485 ºC, 492 ºC and 500 ºC using Bi-mediated growth which was explained by the fact that the QD dimensions became more uniform and homogenous at higher growth temperatures with Bi atoms suppressing the formation of larger dislocated islands. The dot areal density usually decreases at lower growth temperatures and is higher at high temperatures, which reveals essentially the suppression effect of Bi on the surface migration and desorption of In adatoms [18]. The same behavior is observed in our samples, since the dot density decreased from 6.2x10^{10} cm^{-2} to 3.6x10^{10} cm^{-2} from sample B (T_G=495 ºC) to sample C (T_G=467 ºC), however sample D (T_G=435 ºC) shows a higher density of 6.3x10^{10} cm^{-2}. It is worth pointing out that the QD in sample B (T_G=495 ºC) have a bimodal and paired shape, however, in sample C grown at lower temperature (T_G=467 ºC) lateral associations of QD aggregates that contained several disordered large QDs were observed which could explain a lower quantized energy for this structure. Additionally, we have noted a non-monotonic decrease of the optical efficiency for different growth temperature

and its causes will be discussed below in terms of structural defects and areal density of radiative centers.

The PL intensity of Bi mediated growth of QDs grown at the highest temperature is higher than the PL intensity of QDs grown at the lowest temperature, as shown in Figure 13. The higher PL intensity observed for the sample grown at 495 ºC (sample B) could be due to lower density of defects like point defects (e.g., antisites, interstitials, or vacancies) or dislocated islands formed at the higher growth temperature than the lower growth temperature. These defects could be due to some distortion caused by Bi atoms which might exceed the critical strain to generate these defects [32]. This argument is supported by the fact that the PL signal from sample B quenches at a temperature of 140K (not shown here), which is higher than samples C and D, as well as the structural data show a higher QD density for sample B. On the other hand, a non-monotonic decrease of the PL intensity as the growth temperature decreases is observed in these spectra. In particular, sample C (grown at 467 ºC) exhibits the lowest PL intensity as compared to samples grown at 495 ºC and 435 ºC. Although the density of defects, which act as nonradiative recombination centers, increases with decreasing growth temperature, this effect alone cannot fully explain the reduction of PL at 467 ºC. Since PL intensity must also be proportional to the areal density of the radiative centers and all samples were submitted to the same experimental conditions (area beam spot and laser power excitation) the main physical mechanism that may be responsible for the PL local minimum is the areal density. Furthermore, although we have observed a monotonic trend in QD areal density as discussed in AFM and TEM sections, sample C present lateral associations of QD with a number of QDs from 2 to 8. We point out that the lateral associations of QD have a reduced effective area per QD when compared to individual (samples A and D) or bimodal QDs (sample B), since there is an aggregate and merge of individual QDs. Using these arguments, the PL intensity for sample C is expected to have a lower PL intensity than predicted by our estimated QD density and the nonmonotonic behaviour for PL intensity which is well understood.

Furthermore, the narrower PL peaks with FWHM of 27.0 and 25.5 meV at 10K occur for sample B and C, respectively. As discussed before, the distribution of the QD height on the surface of the samples (Fig. 8) shows that for Bi-mediated samples, the distribution became significantly narrower as compared with the control sample A. For sample B (bimodal) and sample C (lateral associations of QD aggregates) the height distributions are similar and narrower than sample A, which agrees with the observed narrower PL FWHM for Bi-mediated samples (Fig. 12 and Fig. 14), since FWHM inversely correlate with QD size and shape uniformity [33, 34]. The FWHM can increase, however, when the QDs become more inhomogeneous, in terms of size, shape or defects. This seems the case for sample D which has the highest PL FWHM of 38.5 meV at 10K, despite that its growth temperature was the lowest and its QD height distribution the narrowest. This indicates that the determining factor for this highest FWHM value could be due to the increase in the concentration of point defects during low-temperature growth and the consequent increased density of tail states in the QDs, since Bi surfactant effect is supressed as the temperature growth is decreased.

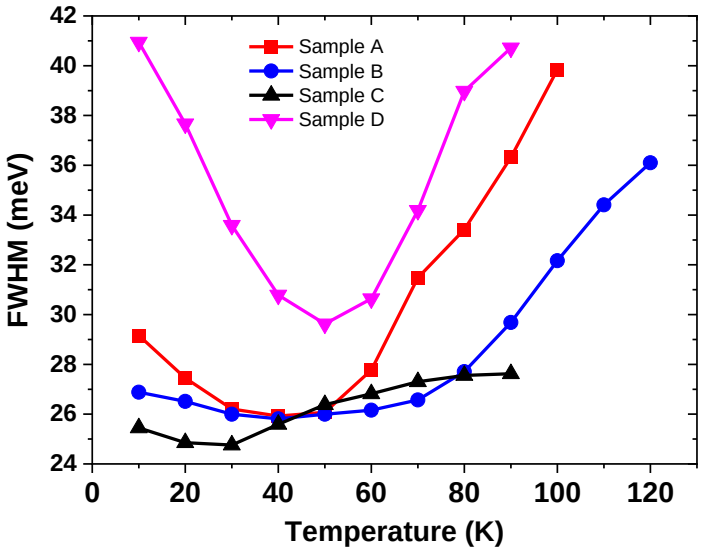

Figure 14: FWHM as a function of temperature for $In_{0.52}Ga_{0.48}As/GaAs$ QDs grown at different temperatures using Bi as surfactant: sample B (T_G=495 ^oC), sample C (T_G=467 ^oC) and sample D (T_G=435 ^oC) measured at 10K and P_{EXC}=25mW. Sample A (control sample without Bi) was grown at T_G=495 ^oC.

Figure 14 shows the PL FWHM versus temperature for InGaAs/GaAs QDs grown at different temperatures using Bi as surfactant (samples labelled B, C and D) and the QD control sample grown without Bi at T_G=495 ^oC (Sample A) for comparison purposes. All samples show a similar behaviour, i.e. the PL FWHM decreases and increases as the sample temperature is increased. However, sample D which is grown at the lowest temperature of 435 ^oC shows the largest FWHM variation and has the highest FWHM at all temperatures. Samples B and C (grown at 495 ^oC and 467 ^oC) have similar FWHM in the temperature range 10-90 K. However, only the sample grown at the highest temperature (sample A) exhibit PL signal up to 120K, meaning that it has the highest optical efficiency. This temperature dependent FWHM behaviour for all samples grown with Bi was reported for InGaAs QDs, which is considered a typical characteristic of this material, and the reduction of the PL FWHM is generally attributed to the carrier thermal redistribution amongst QDs with different sizes as explained in the previous section. It is worth pointing out that the local minimum of the FWHM at ~50K for sample D may represent again the existence of tail states. At lower temperatures < 50 K, tail states are empty at thermal equilibrium (TE) and the photogenerated carriers can recombine from these empty states. As temperature increases up to ~50 K, thermally generated carriers occupy the tail states, hence only the extended QD states are available for recombination. As the temperature increases further, the diffusion length of the photogenerated carriers increases, permitting them to diffuse between quantum dots of different sizes and between localized states, resulting in an increased broadening of PL spectra (i. e. increasing the FWHM value). However, samples B and C show an insignificant FWHM variation of ~2 meV and 3 meV, respectively, between 10 K and 90 K. In contrast, sample D has the highest variation of FWHM of 12.5 meV between 10 K and 50 K. This is probably due to the energy transfer barrier of QDs which is higher in sample B and sample C than in sample D. In general, our results indicate that an increase in the growth

temperature of QDs results in a significant optical improvement and therefore, the optimum temperature for Bi-assisted growth in the scope of the QDs' optical properties is 495°C.

CONCLUSIONS

In summary, the structural, morphological and optical properties of self-assembled $In_{0.52}Ga_{0.48}As$ QDs grown by MBE on GaAs substrates at various growth temperatures with and without exposure to bismuth flux have been investigated using AFM, SEM, TEM and PL techniques. Our samples evidenced the formation of QDs for all growth temperatures used in this work. It was also observed that the PL intensity from QDs is enhanced by ~ 1.7 times by introducing Bi as a surfactant as compared to InGaAs/GaAs control sample grown without Bi. In addition, a red-shift of the PL peak energy of about 40 meV was also observed when the InGaAs QDs were grown by using Bi as a surfactant evidencing that Bi affects considerably the size of QDs. Furthermore, the QDs grown with Bi as a surfactant exhibited a higher degree of size uniformity as demonstrated by the observation of narrower FWHM of the PL peaks. The PL peak redshifts with lower growth temperatures and this could be due primarily to an increase of the size of QDs. This trend is essentially the result of the suppression of Bi surfactant effect on the surface migration and desorption of In adatoms. In addition, the optical efficiency of InGaAs QDs grown under a Bi flux at 467 ^{o}C was found to be lower than samples grown at 495 ^{o}C and 435 ^{o}C. Our results show that the growth temperature of 495 ^{o}C was found to be optimal in terms of optical efficiency. All the obtained results evidence that the use of Bi surfactant is a promising procedure to control the morphology of QDs and improve their optical properties which are essential for future development of photonic and optoelectronic devices.

ACKNOWLEDGMENTS

The authors would like to thank one of the unknown reviewers for bringing up the point of the inadequate use of the anisotropy expression to explain the change of the FWHM of samples D,

and for offering an alternative to explain the observed "notched" shape of the PL FHWM using the existence of tail states. The authors are grateful to A.A. Rudenko for SEM research. The work has been supported by “Fundação de Amparo a Pesquisa do Estado de São Paulo” (Fapesp) (grants no. 19/23488-5 and 19/07442-5) and Conselho Nacional de Desenvolvimento Científico e Tecnológico (CNPQ) (grants 426634/2018-7 and 311678/2020-3).

REFERENCES

[1] K. Akahane and N. Yamamoto, Physica E 42, 2735 (2010).

[2] P. B. Joyce, T. J. Krzyzewski, G. R. Bell, T. S. Jones, S. Malik, D. Childs, and R. Murray, Phys. Rev. B 62, 10891 (2000).

[3] H. Saito, K. Nishi, and S. Sugou, Appl. Phys. Lett. 74, 1224 (1999).

[4] S. Kiravittaya, Y. Nakamura, and O. G. Schmidt, Physica E 13, 224 (2002).

[5] J. M. Garcia, G. Medeiros-Ribeiro, K. Schmidt, T. Ngo, J. L. Feng, A. Lorke, J. Kotthaus, and P. M. Petroff, Appl. Phys. Lett. 71, 2014 (1997).

[6] V. D. Dasika, J. D. Song, W. J. Choi, N. K. Cho, J. I. Lee, and R. S. Goldman, Appl. Phys. Lett. 95, 163114 (2009).

[7] J. Massies and N. Grandjean, Phys. Rev. B 48, 8502 (1993).

[8] D. Guimard, M. Nishioka, S. Tsukamoto, and Y. Arakawa, J. Cryst. Growth 298, 548 (2007).

[9] N. Kakuda, T. Yoshida, and K. Yamaguchi, Appl. Surf. Sci. 254, 8050 (2008).

[10] B. N. Zvonkov, I. A. Karpovich, N. V. Baidus, D. O. Filatov, S. V. Morozov and Y. Gushina. Nanotechnology 11, 221 (2000).

[11] H. Okamoto, T. Tawara, H. Gotoh, H. Kamada, T. Sogawa, Jpn. J. Appl. Phys., 49, 6S (2010).

[12] D. Fan, Z. Zeng, V.G. Dorogan, Y. Hirono, C. Li, Y.I. Mazur, S.-Q. Yu, S.R. Johnson, Z.M. Wang, G.J Salamo, J. Mater. Sci. 24, 1635 (2013).

[13] D. Kandel and E. Kaxiras, Solid State Phys. 54, 219 (1999).

[14] T. F. Kuech, AIP Conf. Proc. 916, 288 (2007).

[15] A. Duzik, J. C. Thomas, J. M. Millunchick, J. Lång, M. P. J. Punkkinen, and P. Laukkanen, Surf. Sci. 606, 1203 (2012).

[16] M. R. Pillai, S.S. Kim, S. T. Ho, and S. A. Barnett. Journal of Vacuum Science and Technology B 18, 1232 (2000).

[17] V.D. Dasika, E.M. Krivoy, H.P.Nair, S. J. Maddox, W. ParkK, D. Jung, M. L. Lee, E. T. Yu and S. R. Bank, Appl. Phys. Lett. 105, 253104 (2014).

[18] X.Y. Chen, Y.Gu, Y.J. Ma, S.M. Chen, M. C.Tang,Y. Y. Zhang, X.Z. Yu, P. Wang, J. Zhang, J. Wu, H.Y Liu and Y. G. Zhang, Mater. Res. Express 6, 015046 (2019).

[19] R. B. Lewis, P. Corfdir, H. Li, J. Herranz, C. Pfüller, O. Brandt, and L. Geelhaar. Phys. Rev. Lett. 119, 086101 (2017).

[20] L Wang, W. Pan, X. C., X. Wu, J. Shao and S. Wang, Optical Materials Express 7 (12), 4249 (2017).

[21] R. B. Lewis, A. Trampert, E. Luna, J. Herranz, C. Pfüller and L. Geelhaar, Semicond. Sci. Technol. 34, 105016 (2019).

[22] S. A. Mintairov, V. V. Evstropov, N. A. Kalyuzhnyy, M. V. Maximov, M. A. Mintairov, A. M. Nadtochiy, N. V. Pavlov, M. Z. Shvarts and A. E. Zhukov, Appl. Phys. Exp. 13, 1 (2020).

[23] F. Bastiman et al. Journal of Crystal Growth 341, 19 (2012).

[24] M. V. Maximov, A. F. Tsatsul'nikov, B. V. Volovik, D. A. Bedarev, A. Yu. Egorov, A. E. Zhukov, A. R. Kovsh, N. A. Bert, V. M. Ustinov, P. S. Kop'ev, and Zh. I. Alferov, Appl. Phys. Lett. 75, 2347 (1999).

[25] T. D. Park, J. S. Colton, J. K. Farrer, H. Yang, and D. J. Kimet, AIP Advances 4, 127142 (2014).

[26] Q. Gong, P. Offermans, R. Nötzel, P. M. Koenraad, and J. H. Wolter, Appl. Phys. Lett. 85, 5697 (2004).

[27] M. Syperek, M. Baranowski, G. Sek, J. Misiewicz, A. Loffler, S. Hofling, S. Reitzenstein, M. Kamp, and A. Forchel, Physical Review, B 87,125305 (2013).

[28] Yu. I. Mazur, B. L. Liang, Zh. M. Wang, G. G. Tarasov, D. Guzun, and G. J. Salamo, J. Appl. Phys. 101(1), 014301 (2007).

[29] A. Hospodková, J. Vyskočil, J. Pangrác, J. Oswald, E. Hulicius and K. Kuldová, Surf. Sci. 604, 318 (2010).

[30] A. D. Utrilla, D. F. Grossi, F. D. Reyes, A. Gonzalo, V. Braza, T. Ben, D. González, A. Guzman, A. Hierro, P. M. Koenraad, J. M. Ulloa, Appl. Surf. Sci. 444, 260 (2018).

[31] T. Matsuura, T. Miyamoto and F. Koyama, Appl. Phys. Lett. 88, 183109 (2006).

[32] D.F. Reyes, D. González, F. Bastiman, L. Dominguez, C.J. Hunter, E. Guerrero, M.A. Roldan, A. Mayoral, J.P.R. David, D.L. Sales, Appl. Phys. Express, 6, 042103 (2013).

[33] R. P. Mirin, K. L. Silverman, D. H. Christensen, and A. Roshko. J. Vac. Sci. Technol. B 18, (3) 1510 (2000).

[34] B. Liang, Q. Yuan, L. Su, Y. Wang, Y. Guo, S. Wang, G. Fu, E. Marega, Y. I. Mazur, M. E. Ware, and G. Salamo, Optics Express 26 (18) 23107 (2018).

[35] M. Yoshimoto, K. Oe. Molecular beam epitaxy of GaAsBi and related quaternary alloys, in Molecular Beam Epitaxy, M. Henini, Eds., Elsevier, Oxford (2013); pp. 159–170.

[36] K. K. Nagaraja, Y. A. Mityagin, M. P. Telenkov & I. P. Kazakov GaAs(1-x)Bix: A Promising Material for Optoelectronics Applications, Critical Reviews in Solid State and Materials Sciences, 42:3, 239-265 (2017)

[37] V. V. Preobrazhenskii, M. A . Putyato, and B. R. Semyagin, Semiconductors 36, 837 (2002).

[38] R. D. Richards, F. Bastiman, C. J. Hunter, D. F. Mendes, A. R. Mohmad, J. S. Roberts, J. P. R. David, Journal of Crystal Growth 390, 120 (2014)